



Effects of dislocation arrangement and character on the work hardening of lath martensitic steels

Hiroyuki Dannoshita^{a,b,*}, Hiroshi Hasegawa^c, Sho Higuchi^c, Hiroshi Matsuda^c, Wu Gong^d, Takuro Kawasaki^d, Stefanus Harjo^d, Osamu Umezawa^{e,f}

^a Graduate School of Engineering Science, Yokohama National University, 79-5 Tokiwadai, Hodogaya-ku, Yokohama 240-8501, Japan

^b Research Fellow of Japan Society for the Promotion of Science DC, Japan

^c Steel Research Laboratory, JFE Steel Corporation, Minamiwatarida-cho, Kawasaki-ku, Kawasaki 210-0855, Japan

^d J-PARC Center, Japan Atomic Energy Agency, Tokai-mura, Naka-gun, Ibaraki 319-1195, Japan

^e Faculty of Engineering, Yokohama National University, 79-5 Tokiwadai, Hodogaya-ku, Yokohama 240-8501, Japan

^f Center of Advanced Innovation Technologies, Vysoká škola Báňská - Technical University of Ostrava, 17. listopadu 15, Ostrava-Poruba 708 33, Czech Republic

ARTICLE INFO

Keywords:

Martensitic steels
Work hardening
Neutron diffraction
Dislocation characteristics
Line profile analysis

ABSTRACT

Work-hardening behavior of a lath martensitic Fe–18Ni alloy during tensile deformation is discussed based on the Taylor's equation. The dislocation characteristics are monitored using *in situ* neutron diffraction. In the specimens of as-quenched (AQ) and tempered at 573 K (T573), the dislocations are extremely dense and randomly arranged. The dislocations in AQ and T573 form dislocation cells as deformation progresses. Consequently, a composite condition comprising cell walls and cell interiors is formed, and the coefficient α in the Taylor's equation increases. Cells are already present in the specimen tempered at 773 K (T773), which has a low dislocation density and a large fraction of edge-type dislocations. As deformation continues, the dislocation density of T773 increases, its cell size decreases, and its composite condition become stronger. Simultaneously, the edge-type dislocation fraction decreases, keeping α unchanged. Thus, both the dislocation arrangement and character affected α , thereby affecting the work-hardening behavior.

The work-hardening behavior of metallic materials is generally expressed using the Taylor's equation [1] where the increment of flow stress ($\Delta\sigma$) is proportional to the square root of the dislocation density (ρ).

$$\Delta\sigma = M_T \alpha G b \sqrt{\rho}, \quad (1)$$

where M_T , α , G , and b are the average Taylor factor, a geometrical coefficient, the shear modulus, and the Burgers vector, respectively. As-quenched lath martensitic steels have an extremely high work-hardening rate. The dislocation densities of the as-quenched martensitic steels hardly change during their deformation; however, the dislocation arrangement changes from a random arrangement to a correlated configuration during the deformation at room temperature [2–4]. The change in the dislocation arrangement can be expressed using the dimensionless parameter M^* , a product of the radius of the strain field produced by the dislocation (R_c^*) and $\sqrt{\rho}$ (i.e., $M^* = R_c^* \sqrt{\rho}$) [5]. The evolution of the dislocation substructure during the work hardening of

lath martensitic steels was confirmed using transmission electron microscopy (TEM) [6]. Mughrabi [7] claimed that coefficient α in Eq. (1) is affected by the dislocation structure and arrangement. Thus, the variation of M^* is a factor that can be used to explain the work-hardening behavior, as indicated by the variation of α [2–4].

The variation of α during deformation of the steels has been demonstrated using *in situ* neutron diffraction measurements combined with line profile analysis [3,8,9] and can be explained using the Mughrabi's composite model [10]; α changed with deformation as dislocation cells formed and the heterogeneity of the dislocation distribution changed. In Mughrabi's composite model, α depends on the volume fractions of the dislocation-rich cell walls (f_w) and dislocation-poor cell interior regions (f_c):

$$\alpha = 2\alpha_{\text{hom}} \sqrt{f_c f_w}, \quad (2)$$

where α_{hom} is the value of α when dislocations distribute homogeneously satisfying the conditions $0.35 < \alpha_{\text{hom}} < 0.4$ [10] or $\alpha_{\text{hom}} = 0.45$

* Corresponding author at: Graduate School of Engineering Science, Yokohama National University, 79-5 Tokiwadai, Hodogaya, Yokohama 240-8501, Japan.

E-mail address: dannoshita-hiroyuki-cz@ynu.jp (H. Dannoshita).

[9]. According to this model, the homogeneous dislocation distribution indicates the equivalent values of f_C and f_W ($f_C = f_W = 0.5$), and the value of f_W is in a range of 0 to 0.5. The α of an AISI-316 stainless steel varied during deformation depending on the $[hkl]$ orientation owing to dislocation structure evolution [9]; consequently α was equal to 0.23 ± 0.03 and 0.47 ± 0.03 for the $[hkl]$ -oriented grains under favorable and unfavorable cell-forming conditions, respectively.

The increase in α during deformation of lath martensitic steels has been linked to the formation of dislocation cells and the change in M^* in order to relate it to Eq. (2) [3]. Dislocation cell walls are hard microstructural components, whereas cell interiors are soft components [7, 11]; edge dislocations are the main components of the dislocation cell walls, whereas screw components are those of the cell interiors [12,13]. The Vickers hardness of steels increases when the fraction of edge dislocations (f_{edge}) becomes larger than that of screw dislocations (f_{screw}) [14]. Thus, the evolution of the dislocation character in lath martensitic steels during deformation [4] may also affect α . However, detailed studies are yet to be conducted on the effect of the dislocation arrangement and character on the work-hardening behavior and the change in the α value of metallic materials, especially lath martensitic steels, during deformation.

This study attempted to clarify the effects of dislocation arrangement and character on the work-hardening behavior of a lath martensitic Fe-18 mass%Ni alloy, particularly on coefficient α in the Taylor's equation. Specimens with an ultralow-carbon content were used in this study to exclude the effect of carbon on the dislocation characteristics and their major constituent phase after quenching to below room temperature was martensite having the body-centered cubic structure. Three types of specimens with different initial dislocation characteristics were prepared as follows. All three specimens were first austenitized at 1173 K for 1.8 ks, water-quenched and then sub-zero treated at 77 K for 1.8 ks (AQ) to prepare the full martensite sample. The AQ samples were subsequently tempered at 573 and 773 K for 3.6 ks, and then they were water-quenched (T573 and T773, respectively). The full martensite condition was kept in the T573, but in the T773, the presence of a tiny amount of austenite with 1.5 mass% was confirmed from the neutron

diffraction pattern and the microscopy observations. The tiny austenite is likely because of the reverted austenite transformation during tempering at 773 K [4]. The effect of the austenitic phase on the strength in the T773 can however be neglectable owing to the quite small amount of austenite because no significant changes were detected in terms of both the volume fraction and microstructural evolution [4]. *In situ* neutron diffraction measurements were performed at room temperature during the tensile deformation of the specimens using the engineering materials diffractometer TAKUMI available at Japan Proton Accelerator Research Complex [15]. The tensile strains were increased in steps to arbitrary values after which they were unloaded, and the diffraction profile data for the line profile analysis were obtained. The convolutional-multiple-whole-profile procedure [16,17] was used to obtain the dislocation characteristics ρ , f_{screw} ($f_{screw} + f_{edge} = 1$), M^* , and area-weighted average crystallite size ($\langle x \rangle_{area}$). The details about specimen preparation, the conditions of the tensile test, and several constants required for the line profile analysis have been described in our previous paper [4].

Fig. 1 shows the changes in the values of the true stress, ρ , f_{screw} , and α during tensile deformation. The true stress–strain curves shown in Fig. 1(a)–(c) were drawn up to the point where the nominal stress reached its maximum value; thus, the last plots of ρ , f_{screw} , and α depict their eventual states immediately before necking. Although ρ in the AQ remained unchanged, the true stress–strain curve indicates that work hardening occurred (Fig. 1(a)). By contrast, ρ in the T773 increased, although the flow stress remained a plateau (Fig. 1(c)). These behaviors are difficult to explain using Eq. (1). Meanwhile, f_{screw} in the T773 increased at the beginning of deformation (Fig. 1(f)), whereas that in the AQ and T573 hardly changed (Fig. 1(d)–(e)). The values of α shown in Fig. 1(g)–(i) were calculated using Eq. (1), the values of $\Delta\sigma$ and ρ shown in Fig. 1(a)–(c), and the other constants described in our previous paper [4]. In the AQ and T573, α started to rapidly increase as deformation started and then tended to converge at approximately 0.3. By contrast, the α of the T773 remained at approximately 0.35 throughout the deformation.

Fig. 2(a) shows the microstructural parameters and evolutions of

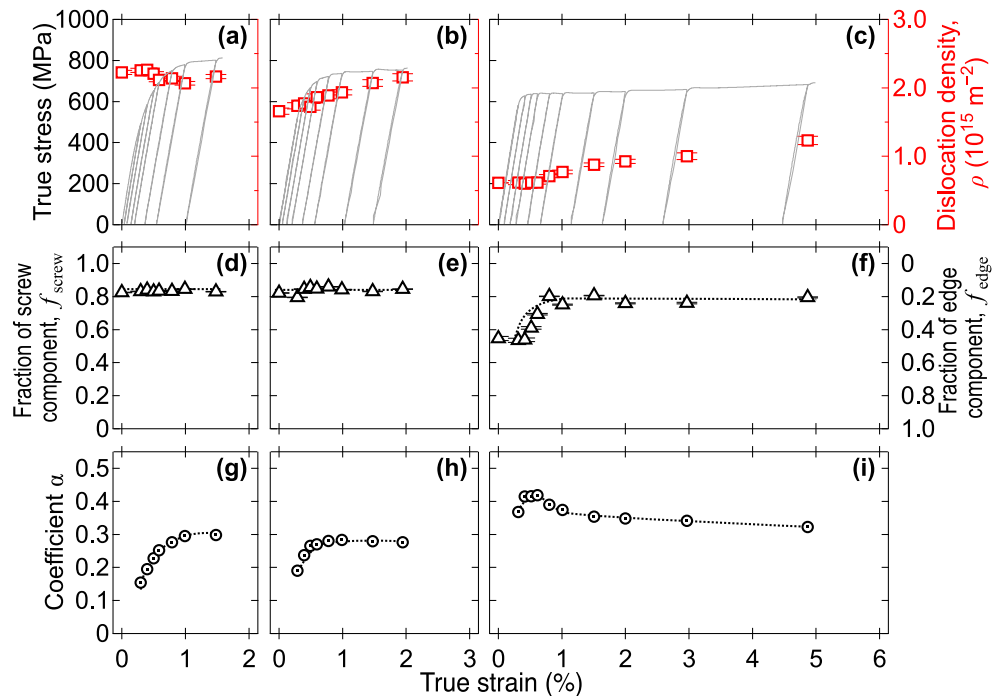


Fig. 1. Changes in the (a)–(c) true stresses and dislocation densities, (d)–(f) fractions of edge and screw dislocations (i.e. f_{screw} and f_{edge}), and (g)–(i) α values during tensile deformation, of the three specimens. The subfigures (a), (d), and (g); (b), (e), and (h); and (c), (f), and (i) refer to the specimens AQ, T573, and T773, respectively.

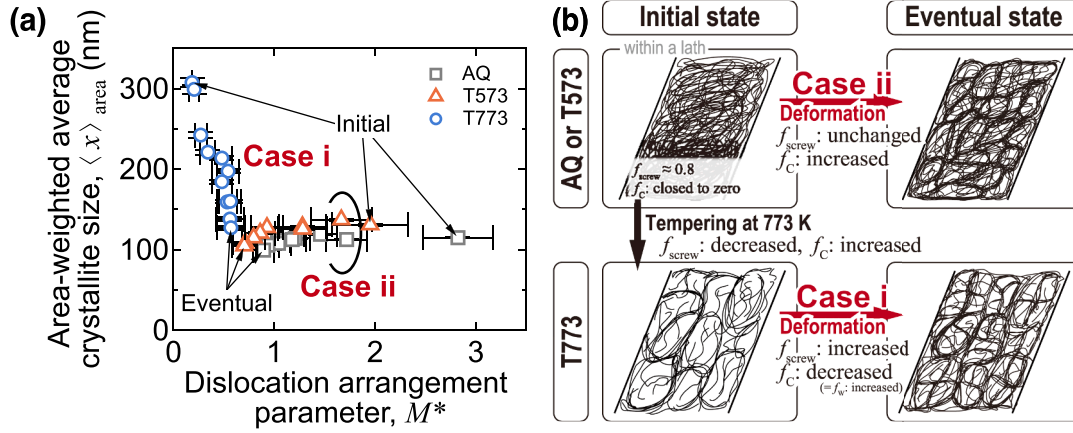


Fig. 2. Evolution of dislocation characteristics with deformation: (a) specimen categorization based on the relationship between M^* and $\langle x \rangle_{\text{area}}$ during tensile deformation and (b) schematic of the dislocation structures within a martensitic lath of AQ and T573 (Case ii), and T773 (Case i), caused by deformations.

each specimen. Two types of relationships were observed between $\langle x \rangle_{\text{area}}$ and M^* : In Case i (T773), $\langle x \rangle_{\text{area}}$ decreased as M^* slightly increased, and in Case ii (AQ and T573), $\langle x \rangle_{\text{area}}$ slightly decreased as M^* drastically decreased. In Case i, α remained almost unchanged (Fig. 1 (i)), and in Case ii, α increased (Fig. 1 (g) and (h)). When M^* is higher or lower than one, the dislocation interaction is weak or strong, respectively, thus indicating a random or correlated arrangement of dislocations, such as a dislocation cell formation, respectively [5]. $\langle x \rangle_{\text{area}}$ has a high correlation with the size of a region that has an extremely low crystal-defect density, such as dislocation cell interiors [18]. Thus, f_{C} and f_{W} can indirectly be represented by M^* and $\langle x \rangle_{\text{area}}$. Consequently, the evolution of the microstructure of each case can be illustrated as shown in Fig. 2(b). We focused on the changes in two types of fractions, namely $f_{\text{C}} (= 1 - f_{\text{W}})$ and $f_{\text{screw}} (= 1 - f_{\text{edge}})$, which cause α to change, to explain the work-hardening behavior of lath martensitic steels. α can be considered a geometrical coefficient contributing to the strength increment per dislocation unit length, which could get affected by both dislocation arrangement and character.

In Case i (T773), the decrease in the dislocation cell size was estimated using $\langle x \rangle_{\text{area}}$. ρ in the T773, however, increased. This tendency has been confirmed using electron channeling contrast imaging (ECCI) [4]. The decrease in the dislocation cell size and multiplication of the dislocations resulted in an increase in f_{W} during deformation (Fig. 2(b)). Thus, according to Mughrabi's composite model (Eq. (2)), α should increase during deformation. However, the α of the T773 remained almost unchanged during deformation despite the increase in f_{W} . Thus, as indicated below, we had to consider another factor in addition to f_{W} and f_{C} to explain Case i.

Based on the dislocation theory, the elastic strain energy per unit length of dislocation (E_{el}) can be expressed as follows.

$$E_{\text{el}} = \frac{Gb^2}{4\pi k} \ln\left(\frac{R}{r_0}\right), \quad (3)$$

where R and r_0 are the radius of the stress field caused by a dislocation and that of the dislocation core, respectively [19]. k is a parameter that depends on the dislocation character and $k = 1 - \nu$ for an edge dislocation and $k = 1$ for a screw dislocation, where ν is the Poisson's ratio. In the case where the elastic fields are superposed by both edge and screw components, E_{el} and k can be expressed using the sum of the edge and screw dislocation energies with b replaced by $b\sin\varphi$ and $b\cos\varphi$, respectively [19]:

$$E_{\text{el}}(\text{mixed}) = \frac{Gb^2(1 - \nu\cos^2\varphi)}{4\pi(1 - \nu)} \ln\left(\frac{R}{r_0}\right), \quad (4)$$

and thus, $k = \frac{1 - \nu}{1 - \nu\cos^2\varphi}$,

where φ is the angle between the direction of the Burgers vector and dislocation line whose direction depends on the ratio of the edge and screw components.

The concept of φ is illustrated in Fig. 3(a) as a geometrical relationship between f_{screw} and φ .

$$f_{\text{screw}} = \frac{\cos\varphi}{\cos\varphi + \sin\varphi} \quad (5)$$

As both k and f_{screw} are functions of φ , k can be expressed as a function of f_{screw} .

$$k = \frac{(\nu - 1)(2f_{\text{screw}}^2 - 2f_{\text{screw}} + 1)}{2f_{\text{screw}} + \nu f_{\text{screw}}^2 - 2f_{\text{screw}}^2 - 1} \quad (6)$$

Fig. 3(b) shows the relationship between k and f_{screw} for $\nu = 0.31$, the value of ν of the specimens used in this study [4]. k is most likely to affect α and $\Delta\sigma$ since the externally applied stress is proportional to the line tension of the dislocations. The line tension is generally defined as the increase in E_{el} . The influence of the dislocation character on work hardening can be represented by k .

We proposed a modified composite model, referred to as a double composite model, to express α by multiplying Eq. (2) by $1/k$ as indicated below.

$$\alpha = 2\alpha_{\text{hom}} \sqrt{f_{\text{C}}f_{\text{W}}} \frac{1}{k} \quad (7)$$

Fig. 3(c) shows the α vs. f_{W} curves obtained using Eq. (7) for different values of f_{screw} and α_{hom} of 0.45 [9]. Evidently from the figure, α increases as f_{W} increases. Moreover, when f_{W} remains unchanged, an increase in f_{screw} corresponds to an increase in k and a decrease in α . Fig. 3 (d) shows α as a function of f_{screw} ; evidently, an increase in f_{screw} causes a decrease in α . Thus, Eq. (7) can be used to explain the increase in the hardness of 18Cr–8Ni steel (mass%) owing to an increase in f_{edge} , whereas ρ remained unchanged [14]. By plotting the experimentally evaluated values of α (Fig. 1 (i)) of the initial and eventual states against the related values of f_{screw} as shown in Fig. 3(c) and (d), the refinement of the dislocation cells and multiplication of the dislocations, i.e. increase in f_{W} with deformation, can be understood. The dashed line in Fig. 3(c) shows the α vs. f_{W} curve for $f_{\text{screw}} = 0.8$. The initial value of α on the curve corresponds to $f_{\text{edge}} = f_{\text{screw}}$, whereas its eventual value on the curve corresponds to $f_{\text{screw}} = 0.8$. The simultaneous increase in both f_{W} and f_{screw} would have led α to remain almost unchanged during the deformation.

In Case ii (AQ and T573), at the beginning of deformation, α increased as the applied strain increased. A similar tendency was observed during the tensile deformation of low-carbon martensitic steel

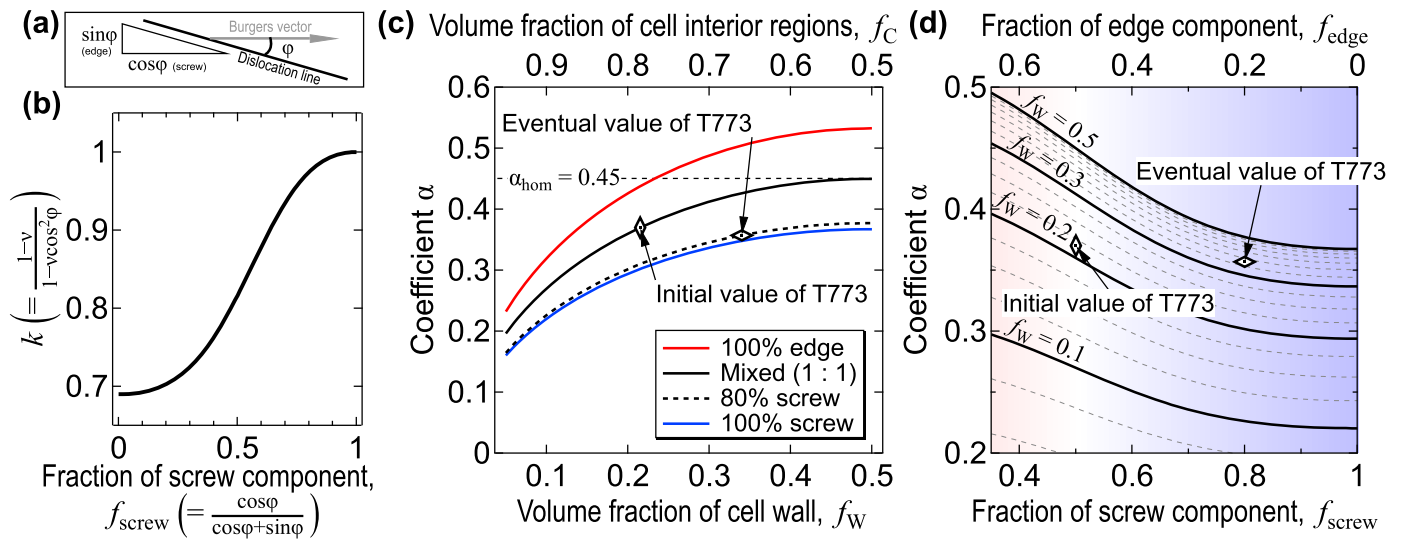


Fig. 3. (a) Schematic showing mixed dislocations and relationships between parameters: (b) k and f_{screw} , (c) f_W (or f_C) and α for different values of k , and (d) f_{screw} (or f_{edge}) and α . The initial and eventual values of α in T773 have been inserted in (c) and (d).

tempered at 473 K [3]; the increase in α was reported to be attributed to the increase in f_W . The increase in f_W occurred with dislocation cell formation, which could be indirectly judged by the decrease in M^* as the deformation progressed. These results appear to follow Mughrabi's composite model (Eq. (2)); that is, an increase in f_W results in an increase in α . However, the extremely high ρ , high M^* , and low $(x)_{\text{area}}$ of the initial state could indicate that the initial f_C value of the AQ/T573 has to be lower than that of the T773. In our previous study that used ECCI [4], no dislocation cells were observed in the AQ and T573 and highly dense and randomly distributed dislocations were observed in them. Therefore, the f_C values of the AQ and T573 before deformation would have been extremely low.

As long as the limit value of f_W is taken as 0.5 in Mughrabi's composite model and f_C of the AQ and T573 remain extremely low, the relationship between α and f_W or f_C in the AQ and T573 is difficult to comprehend. In addition, the effect of the dislocation character on α could be extremely small because f_{screw} remained almost unchanged during deformation; thus, the proposed double composite model (Eq. (7)) cannot be used for Case ii. In Mughrabi's composite model, a dislocation cell wall is defined as a microstructural region with a high dislocation density, and f_W lies in the range from 0.1 to 0.3 [10]. The as-quenched martensitic steel comprises extremely high-density and randomly distributed dislocations [20]. The dislocations with these features is deemed as the microstructure where the major component is the dislocation-cell-wall-like microstructure, thus indicating that f_W can be higher than 0.5. Takaki et al. [21] found a relationship between ρ and f_W using data pertaining to the dislocation cell size and cell wall thickness [22,23]. Accordingly, an f_W larger than 0.5 could be achieved when ρ becomes higher than 10^{15} m^{-2} [21]. Therefore, both f_W and f_C in Mughrabi's composite model can be extended to be between 0 and 1, and a symmetrical curve of α with its highest value at $f_W = f_C = 0.5$ could be obtained, as shown in Fig. 4; this new model is hereinafter to be referred to as an extended composite model. When the initial values of α of the AQ and T573 were plotted on the calculated curve, where $f_{\text{screw}} = 0.8$, the estimated initial f_W was approximately 0.9 (Fig. 4). Thus, the eventual values of α could be attributed to the increase in f_C during deformation. The increase in f_C implies dislocation cell formation within martensitic laths, which has been confirmed using ECCI [4,24] and TEM [2]. Therefore, the inconsistencies observed in the increase in α with the decrease in M^* can be explained using the extended composite model.

In summary, the work-hardening behavior of a lath martensitic Fe-18Ni alloy during its tensile deformation was discussed based on the

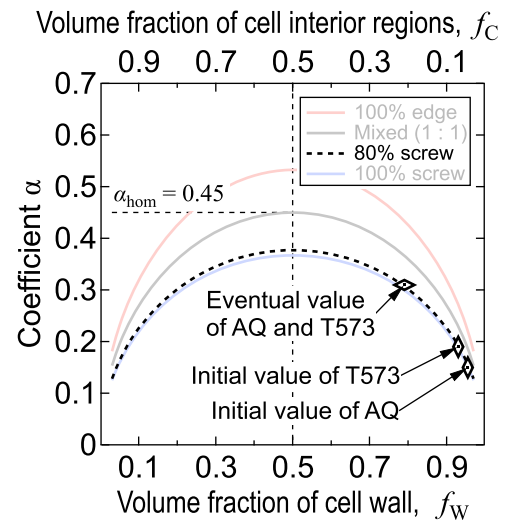


Fig. 4. Relationship between f_W (or f_C) and α value obtained using the extended composite model. The initial and eventual values of α are inserted for AQ and T573.

Taylor's equation and using dislocation characteristics (dislocation density, arrangement, and character) monitored using *in situ* neutron diffraction. Three types of specimens, namely an as-quenched specimen (AQ), an as-quenched specimen tempered at 573 K (T573), and 773 K (T773), were used. The variation of α (a coefficient included in the Taylor's equation) during deformation was related to the evolution of dislocation characteristics, a composite condition related to the formation and evolution of dislocation cells. The initial value of α in the AQ or T573 was extremely small and its eventual value was approximately 0.3. Before deformation began, dislocations with highly dense and random arrangements were assumed to contain mostly cell walls, which evolved to form dislocation cells as deformation progressed. Consequently, cell interiors were formed, *i.e.*, a composite condition was formed and α increased. This behavior can be explained using an extended composite model. The initial value of α in the T773 was above 0.3, subsequently remained almost unchanged during deformation. With high-temperature tempering, dislocations became low in density, comprising a large fraction of edge-type dislocations and formed dislocation cells, *i.e.* a composite condition. With deformation at room

temperature, the dislocation density increased, and cell size decreased in the T773, thus indicating that the composite condition had become stronger. Simultaneously, however, the fraction of edge dislocations decreased, keeping α almost unchanged. By considering the dislocation character in addition to the fraction of cell walls or interiors, the variation of α can be understood, and this behavior can be explained through the proposed double composite model.

Declaration of Competing Interest

The authors declare that they have no known competing financial interests or personal relationships that could have appeared to influence the work reported in this paper.

Acknowledgements

This work was supported by JSPS KAKENHI Grant Numbers JP21J522690 and JP18H05479 and MEXT Program: Data Creation and Utilization Type Material Research and Development (JPMXP1122684766). The experiments were undertaken on a high-resolution time-of-flight neutron diffractometer TAKUMI at the Materials and Life Science Experimental Facility of Japan Proton Accelerator Research Complex (Proposal No. 2019I0019). The authors acknowledge Dr. S. Goto (currently at Central Research Institute of Electric Power Industry) and Ms. D. Thi-Huyen of JFE Steel Corporation for valuable discussions and preparation of samples.

References

- [1] G.I. Taylor, The mechanism of plastic deformation of crystals. Part I.—Theoretical, *Proc. R. Soc. Lond. A* 145 (855) (1934) 388–404.
- [2] D. Akama, T. Tsuchiyama, S. Takaki, Change in dislocation characteristics with cold working in ultralow-carbon martensitic steel, *ISIJ Int.* 56 (9) (2016) 1675–1680.
- [3] S. Harjo, T. Kawasaki, Y. Tomota, W. Gong, K. Aizawa, G. Tichy, Z. Shi, T. Ungár, Work hardening, dislocation structure, and load partitioning in lath martensite determined by *in situ* neutron diffraction line profile analysis, *Metall. Mater. Trans. A* 48 (2017) 4080–4092.
- [4] H. Dannoshita, H. Hasegawa, S. Higuchi, H. Matsuda, W. Gong, T. Kawasaki, S. Harjo, O. Umezawa, Evolution of dislocation structure determined by neutron diffraction line profile analysis during tensile deformation in quenched and tempered martensitic steels, *Mater. Sci. Eng. A* 854 (2022), 143795.
- [5] M. Wilkens, The determination of density and distribution of dislocations in deformed single crystals from broadened X-ray diffraction profiles, *Phys. Status Solidi A* 2 (2) (1970) 359–370.
- [6] J. Cuddy, M. Nabil Bassim, Study of dislocation cell structures from uniaxial deformation of AISI 4340 steel, *Mater. Sci. Eng. A* 113 (1989) 421–429.
- [7] H. Mughrabi, A two-parameter description of heterogeneous dislocation distributions in deformed metal crystals, *Mater. Sci. Eng.* 85 (1987) 15–31.
- [8] T. Ungár, S. Harjo, T. Kawasaki, Y. Tomota, G. Ribárik, Z. Shi, Composite behavior of lath martensite steels induced by plastic strain, a new paradigm for the elastic-plastic response of martensitic steels, *Metall. Mater. Trans. A* 48 (1) (2017) 159–167.
- [9] T. Ungár, A.D. Stoica, G. Tichy, X.L. Wang, Orientation-dependent evolution of the dislocation density in grain populations with different crystallographic orientations relative to the tensile axis in a polycrystalline aggregate of stainless steel, *Acta Mater.* 66 (2014) 251–261.
- [10] H. Mughrabi, The α -factor in the Taylor flow-stress law in monotonic, cyclic and quasi-stationary deformations: dependence on slip mode, dislocation arrangement and density, *Curr. Opin. Solid State Mater. Sci.* 20 (6) (2016) 411–420.
- [11] H. Mughrabi, Dislocation wall and cell structures and long-range internal stresses in deformed metal crystals, *Acta Metall.* 31 (9) (1983) 1367–1379.
- [12] W.D. Nix, J.C. Gibeling, D.A. Hughes, Time-dependent deformation of metals, *Metall. Trans. A* 16 (12) (1985) 2215–2226.
- [13] P. Haasen, A cell theory for stage IV work hardening of metals and semiconductors, *J. Phys.* 50 (18) (1989) 2445–2453.
- [14] T. Shintani, Y. Murata, Evaluation of the dislocation density and dislocation character in cold rolled Type 304 steel determined by profile analysis of X-ray diffraction, *Acta Mater.* 59 (11) (2011) 4314–4322.
- [15] S. Harjo, T. Ito, K. Aizawa, H. Arima, J. Abe, A. Moriai, T. Iwahashi, T. Kamiyama, Current status of engineering materials diffractometer at J-PARC, *Mater. Sci. Forum* 681 (2011) 443–448.
- [16] T. Ungár, Dislocation densities, arrangements and character from X-ray diffraction experiments, *Mater. Sci. Eng. A* 309–310 (2001) 14–22.
- [17] G. Ribárik, J. Gubicza, T. Ungár, Correlation between strength and microstructure of ball-milled Al–Mg alloys determined by X-ray diffraction, *Mater. Sci. Eng. A* 387–389 (1–2 SPEC. ISS) (2004) 343–347.
- [18] T. Ungár, J. Gubicza, G. Ribarik, A. Borbely, Crystallite size distribution and dislocation structure determined by diffraction profile analysis: principles and practical application to cubic and hexagonal crystals, *J. Appl. Crystallogr.* 34 (3) (2001) 298–310.
- [19] D. Hull, D.J. Bacon, Chapter 4 - Elastic Properties of Dislocations, in: D. Hull, D.J. Bacon (Eds.), *Introduction to Dislocations* (5th Edition), Butterworth-Heinemann, Oxford, 2011, pp. 63–83.
- [20] S. Morito, J. Nishikawa, T. Maki, Dislocation density within lath martensite in Fe-C and Fe-Ni alloys, *ISIJ Int.* 43 (9) (2003) 1475–1477.
- [21] S. Takaki, T. Tsuchiyama, Theoretical discussion of dislocation strengthening in cold rolled iron, *Tetsu Hagané* 104 (2) (2018) 117–120.
- [22] Y. Lan, H.J. Klaar, W. Dahl, Evolution of dislocation structures and deformation behavior of iron at different temperatures: part I. strain hardening curves and cellular structure, *Metall. Trans. A* 23 (2) (1992) 537–544.
- [23] Y. Lan, H.J. Klaar, W. Dahl, Evolution of dislocation structures and deformation behavior of iron at different temperatures: part II. dislocation density and theoretical analysis, *Metall. Trans. A* 23 (2) (1992) 545–549.
- [24] M. Shamsujjoha, Evolution of microstructures, dislocation density and arrangement during deformation of low carbon lath martensitic steels, *Mater. Sci. Eng. A* 776 (2020), 139039.